

Dhay Ali Sabur<sup>1</sup>, Majeed Ali Habeeb<sup>2</sup>, Ahmed Hashim<sup>2</sup>

## **Fabrication and Tailoring the Structural and Dielectric Characteristics of GO/Sb<sub>2</sub>O<sub>3</sub>/PMMA/PC Quaternary Nanostructures For Solid State Electronics Nanodevices**

<sup>1</sup>*Department of Optics Techniques, Al-Mustaqbal University College, Babylon, Iraq*

<sup>2</sup>*University of Babylon, College of Education for Pure Sciences, Department of Physics, Iraq, [ahmed\\_taqy@yahoo.com](mailto:ahmed_taqy@yahoo.com)*

In this paper, films of (PMMA-PC/Sb<sub>2</sub>O<sub>3</sub>-GO) quaternary nanostructures were prepared by casting method with different concentrations of Sb<sub>2</sub>O<sub>3</sub>/GO NPs are (0, 1.4 %, 2.8 %, 4.2 %, and 5.6 %). The structural and dielectric characteristics of nanostructures system (PMMA-PC/Sb<sub>2</sub>O<sub>3</sub>-GO) have been explored to use in different solid state electronics nanodevices applications. The morphology of (PMMA-PC/Sb<sub>2</sub>O<sub>3</sub>-GO) nanostructures films was studied using a scanning electron microscope (SEM). SEM images indicate a large number of uniform and coherent aggregates or chunks. The Fourier transform infrared spectroscopy (FTIR) analysis were studied to show the interactions between the Sb<sub>2</sub>O<sub>3</sub>/GO NPs and PMMA/PC blend. The dielectric properties of nanostructures films were investigated in the frequency range (100HZ-5MHZ). The dielectric constant, dielectric loss, and A.C electrical conductivity increase with the concentration of (Sb<sub>2</sub>O<sub>3</sub>-GO) NPs. The dielectric constant and dielectric loss were reduced, whereas electrical conductivity increased with frequency. Finally, results showed the PMMA-PC/Sb<sub>2</sub>O<sub>3</sub>-GO nanostructures may be considered as promising materials for solid state electronics nanodevices.

**Keywords:** nanocomposites, Graphene oxide, dielectric properties, blend, nanodevices.

*Received 26 July 2022; Accepted 9 March 2023.*

### **Introduction**

In recent years, the worldwide community has drawn their consideration towards materials with appropriate and sustainable characteristics. Development of characteristics can be done with a variety of doping substances. The nature and the technique of their fabrication are the factors the most influencing these characteristics. Targeted applications and cost guide researchers on the choice of substances and the technology to be employed in developing the desired devices. Polymers and mainly hybrid composites (organic-inorganic) are attracting growing consideration from researchers as a result of their utilize in numerous industrial sectors [1]. Poly-methylmethacrylate (PMMA) is an significant kind of polymer amid thermoplastics. PMMA is an optically transparent thermoplastic, which is expansively used as a substitute for inorganic glass. PMMA has been prepared using various polymerization

techniques. PMMA is an significant thermoplastic substance with extensive fields in several technological fields due to its unique optical, mechanical, thermal and electrical properties. PMMA is an amorphous polymer with excellent chemical, weather, scratch, and corrosion resistance. It is lightweight, shatter-resistant, and possess favorable processing conditions. PMMA has been used in a range of fields like coatings, additives, sealers, optical fibers, and transparent neutron stoppers [2]. Polycarbonate (PC) has a high degree of transparency. As a result, it may be employed in a variety of industrial applications, including electrical devices, optical fibers, optical storage devices, and glass lenses. However, improving the optical characteristics of polycarbonate is required in contemporary industrial applications. Furthermore, inorganic fillers are promising possibilities for improving the mechanical characteristics, transparency, and toughness of PC without compromising its mechanical qualities. PC appears to be a good host material for a

variety of NPs. Doped Polycarbonate composites containing metal chalcogenides or oxides have distinct optical and structural properties, making them suitable for industrial applications [3]. GO is insulating due to the breaking of the conjugated electronic structure by means of

oxidized functional groups, and it contains permanent defects and disorders. Hence, the electrical characters of GO sheets are dissimilar from those of pristine graphene [4]. Antimony trioxide ( $Sb_2O_3$ ) is used as a catalyst, a retardant, a conductive substance, a functional filler, and an optical material.  $Sb_2O_3$  is also valuable in plastics, paints, adhesives, and textile back coatings as conductive materials and a high-efficiency flame-retardant synergist [5]. This work aims to prepare of (PMMA-PC/ $Sb_2O_3$ -GO) nanocomposite film studying the structural and dielectric properties to use in different electronic devices.

## I. Materials and Method

Polymethylmethacrylate (PMMA), polycarbonate (PC), antimony trioxide ( $Sb_2O_3$ ), and graphene oxide (GO) were employed in this study. The casting technique was used to prepare nanocomposites films (PMMA-PC/ $Sb_2O_3$ -GO). The films were prepared by dissolving 1g of the (PMMA-PC) blend with ratio 80/20 % in

chloroform using a magnetic stirrer. The ( $Sb_2O_3$ -GO) NPs were introduced in the polymeric blend by (1.4%, 2.8%, 4.2%, and 5.8%). The dielectric properties are determined in the frequency range 100Hz-5MHz using an LCR meter.

The dielectric constant ( $\epsilon'$ ) is calculated by [6]:

$$\epsilon' = C_p / C_0 \quad (1)$$

$C_0$  and  $C_p$  are vacuum and parallel capacitances. The dielectric loss ( $\epsilon''$ ) is gives by [6]:

$$\epsilon'' = \epsilon' \cdot D \quad (2)$$

D is the dispersion factor. The A.C conductivity was calculated by [7]:

$$\sigma_{A.C} = W \cdot \epsilon'' \cdot \epsilon_0 \quad (3)$$

w is the angular frequency.

## II. Results and Discussion

Figure (1) indicates the SEM images of (PMMA-PC/ $Sb_2O_3$ -GO) nanocomposites. The compatibility of different polymer components with ( $In_2O_3$ ,  $Sb_2O_3$ ) nanoparticles was investigated using scanning electron

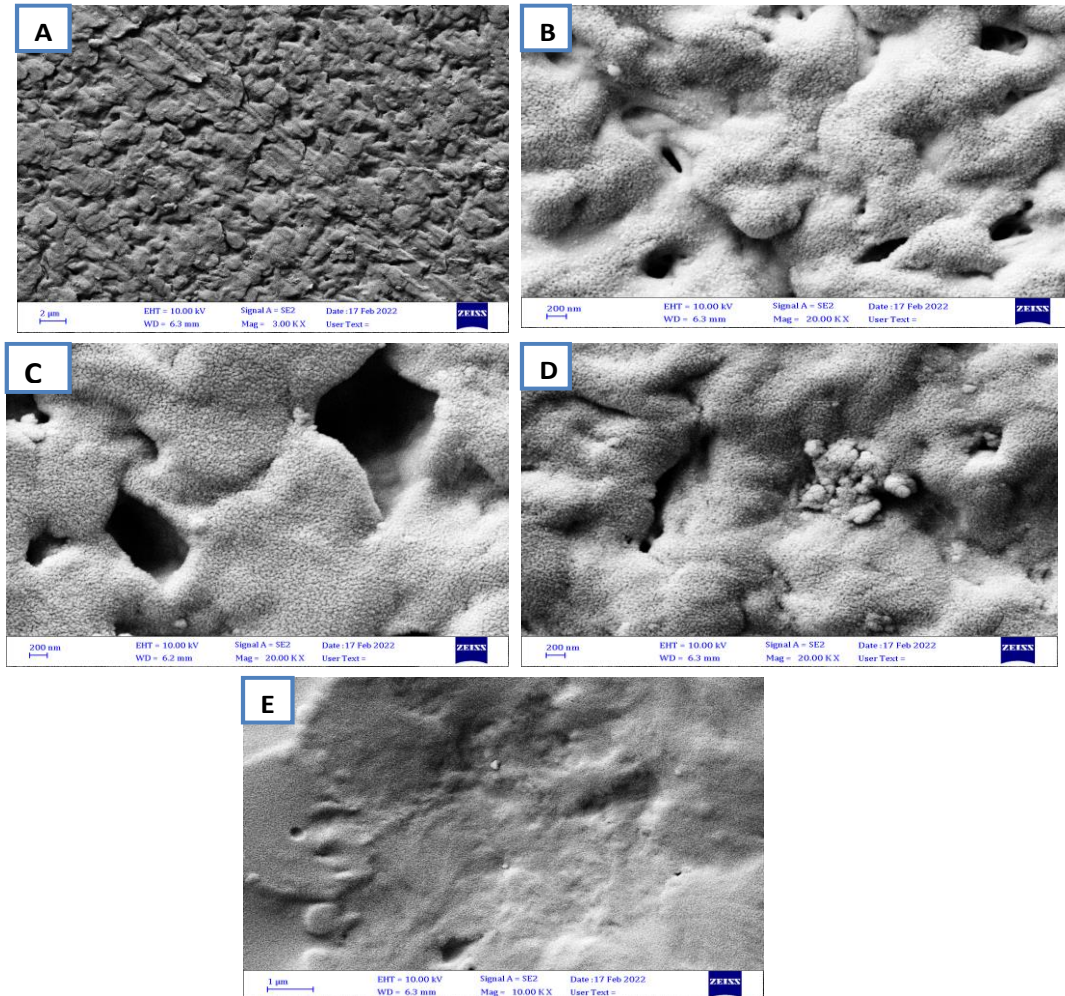


**Fig. 1.** SEM images for (PMMA-PC/ $Sb_2O_3$ -GO) Nanocomposites: (A) for pure (B) for 1.4 wt.%  $Sb_2O_3$ -GO NPs (C) for 2.8 wt.%  $Sb_2O_3$ -GO NPs (D) for 4.2wt.%  $Sb_2O_3$ -GO NPs (E) for 5.6 wt.%  $Sb_2O_3$ -GO NPs.

microscopy. The films have a homogeneous grain distribution at surface morphology, whereas the surfaces of the (PMMA-PC/Sb<sub>2</sub>O<sub>3</sub>-GO) nanocomposites include numerous aggregates or pieces of nanoparticles randomly scattered on the surface. The results are shown when increasing the content of (Sb<sub>2</sub>O<sub>3</sub>-GO) NPs, the number of aggregations on the surface can be increased [8], also the SEM images show the (Sb<sub>2</sub>O<sub>3</sub>-GO) nanoparticles have formed the paths network inside the (PMMA-PC) blend where charge carriers are allowed to pass through this the paths [9]. Figure (2) shows the FTIR spectra of (PC-PMMA-Sb<sub>2</sub>O<sub>3</sub>-GO) nanocomposites at room temperature in the range 4000–500 cm<sup>-1</sup>. These results reveal that there was no chemical interaction between the components in the (PMMA-PC) blends. The transmittance of the carbonyl and methoxyl stretches of PMMA reduced with increasing in PMMA content, while the transmittance of these peaks increased with an increase in PC concentration, according to a detailed examination of the FTIR spectra for these blends. Because no alterations in the peaks of any of these functional groups in the (PMMA-PC) blend spectra suggest the creation of polymer blends, it may be argued that there is no chemical interaction between component polymers. Thus, these are certainly physical blends. The absorption band at around 1723cm<sup>-1</sup> appear C = O stretching band in PMMA. The FTIR bands

at 1434cm<sup>-1</sup> attributed to CH<sub>2</sub> scissoring. O – CH<sub>3</sub> stretching resulted in a peak at 1143.66 cm<sup>-1</sup> rocking made of vibration. while the peak at 749.63 cm<sup>-1</sup> was due to CH<sub>2</sub> rocking made of vibration. Finally, the adding of (Sb<sub>2</sub>O<sub>3</sub> and GO) NPs to the polymer blend results in two noteworthy alterations: modest changes in absorption band intensities and vibrational band intensities in peak at 995.79 cm<sup>-1</sup> and 749cm<sup>-1</sup>. This suggests that the interaction between Sb<sub>2</sub>O<sub>3</sub> and GO NPs and the two polymers has resulted in a decoupling of the corresponding vibrations.

Figure (3) shows the dielectric constant of (PMMA-PC/Sb<sub>2</sub>O<sub>3</sub>-GO) nanocomposites varies with frequency, the dielectric constant values decrease with increasing applied frequency, with increasing frequency causing a decrease in space charge polarization to total polarization, with space charge polarization becoming more contributing to polarization at low frequencies and less contributing with increasing frequency, causing a decrease in dielectric constant values for all samples of (PMMA-PC/Sb<sub>2</sub>O<sub>3</sub>-GO)nanocomposites with polarization. When compared to electronic polarization, ionic polarization reacts somewhat more to changes in field frequencies because the mass of an ion is larger. Figure (4) shows the dielectric constant of (PMMA-PC/Sb<sub>2</sub>O<sub>3</sub>-GO) nanocomposites vary with the Sb<sub>2</sub>O<sub>3</sub>-GO NPs content at 100 Hz, The dielectric constant of (PMMA-PC) blend increases with increased

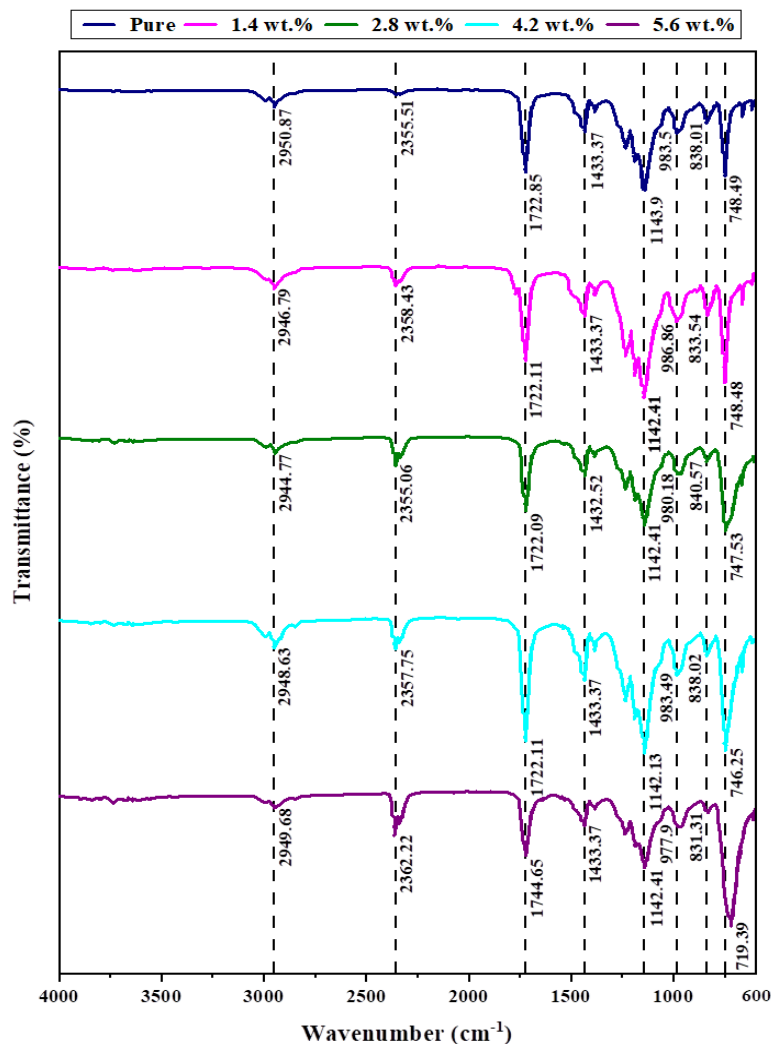


**Fig. 2.** FTIR spectra for (PC-PMMA-Sb<sub>2</sub>O<sub>3</sub>-GO) NPs (A) for (PMMA-PC) blend (B) for 1.4wt% (Sb<sub>2</sub>O<sub>3</sub>-GO) NPs, (C) for 2.8wt% (Sb<sub>2</sub>O<sub>3</sub>-GO) NPs, (D) for 4.2wt% (Sb<sub>2</sub>O<sub>3</sub>-GO) NPs, (E) for 5.8wt% (Sb<sub>2</sub>O<sub>3</sub>-GO) NPs.

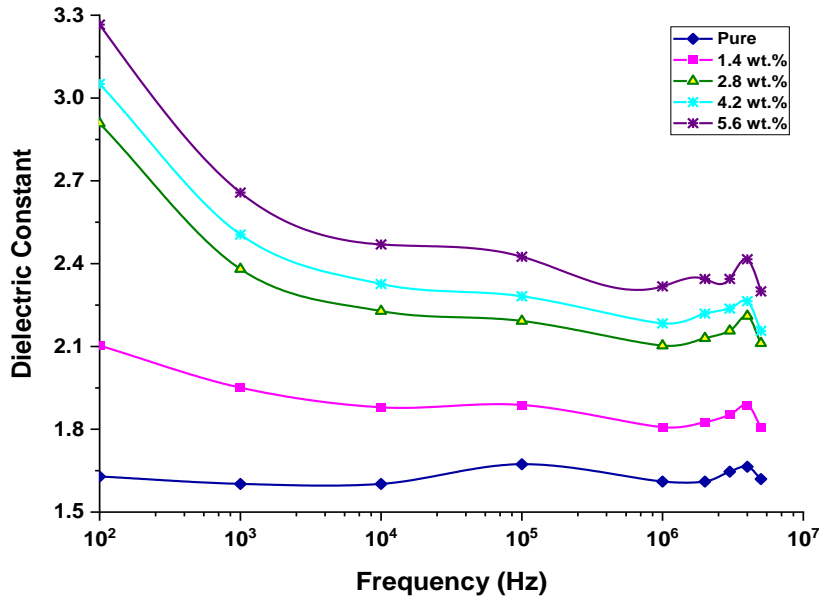


**Fig. 3.** Variation of dielectric constant for (PMMA-PC/Sb<sub>2</sub>O<sub>3</sub>-GO) Nanocomposites with frequency at room temperature.

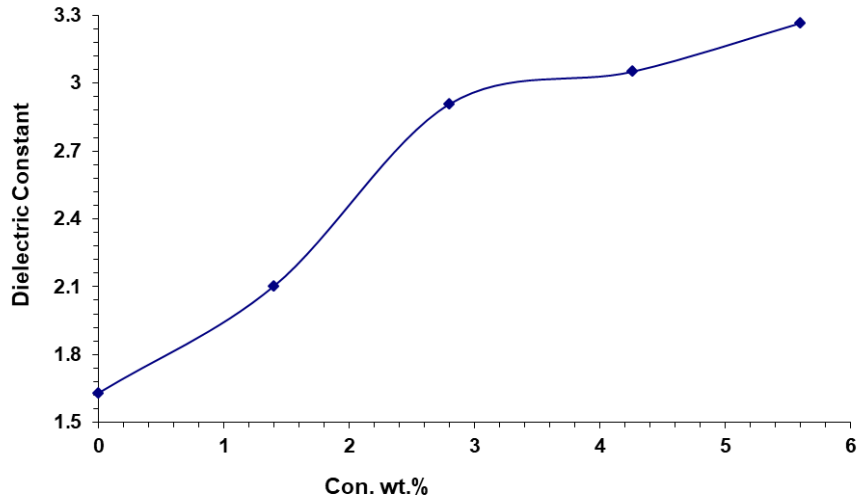


**Fig. 4.** Effect of (Sb<sub>2</sub>O<sub>3</sub>-GO) NPs content on dielectric constant for (PMMA-PC) blend at 100Hz.

concentration of Sb<sub>2</sub>O<sub>3</sub>-GO NPs. This result might be attributed to interfacial polarization inside nanocomposites under an alternating electric field (E1) and, additionally, in charge carriers [10]. Given the high value of the dielectric constant for Sb<sub>2</sub>O<sub>3</sub>-GO NPs, the dielectric constant (PMMA-PC/Sb<sub>2</sub>O<sub>3</sub>-GO) nanocomposites are also high [11].

Figure (5) indicates the dielectric loss with frequency for (PMMA-PC) blend with and without different (Sb<sub>2</sub>O<sub>3</sub>-GO) NPs concentrations. When the frequency is raised, the dielectric loss values for all of the samples tested drop. The creation of free charges occurs at a lower frequency when free charges are generated at the interface between the studied material and the electrode, it also has a maximum value [12]. After a certain frequency value, charge carriers can no longer follow the applied electric field, dielectric loss lowers with increasing frequency, and the fast reduction may be related to polarization for trapped carriers [13]. Figure (6) indicates the dielectric loss increases as the concentration of (Sb<sub>2</sub>O<sub>3</sub>-GO) NPs increases, a result ascribed to a rise in charge carriers

inside the nanocomposites. Furthermore, the increase in dielectric loss with increasing concentrations of (Sb<sub>2</sub>O<sub>3</sub>-GO) NPs might be due to the creation of a path of conductive, which would result in leakage current [14,15].

Figure (7) shows the A.C electrical conductivity of (PMMA-PC/Sb<sub>2</sub>O<sub>3</sub>-GO) nanocomposites changes with the frequency of the electric field at room temperature. Because of charge-carrier mobility and ion hopping from the cluster, A.C electrical conductivity improves with higher electric field frequency. At low frequencies, charge buildup occurs at the electrode-electrolyte interface, resulting in reduced ion mobility and electrical conductivity [16]. Because charge-carrier mobility rises as the frequency field increases [17], the electrical conductivity of nanocomposites improves which is agree with [18-20]. The behavior of A.C electrical conductivity of (PMMA-PC) with Sb<sub>2</sub>O<sub>3</sub>-GO NPs contents is shown in Figure (8). Because of the composition of dopant NPs, the A.C electrical conductivity of the PMMA -PC blend improves with increased Sb<sub>2</sub>O<sub>3</sub>-GO NPs concentration,

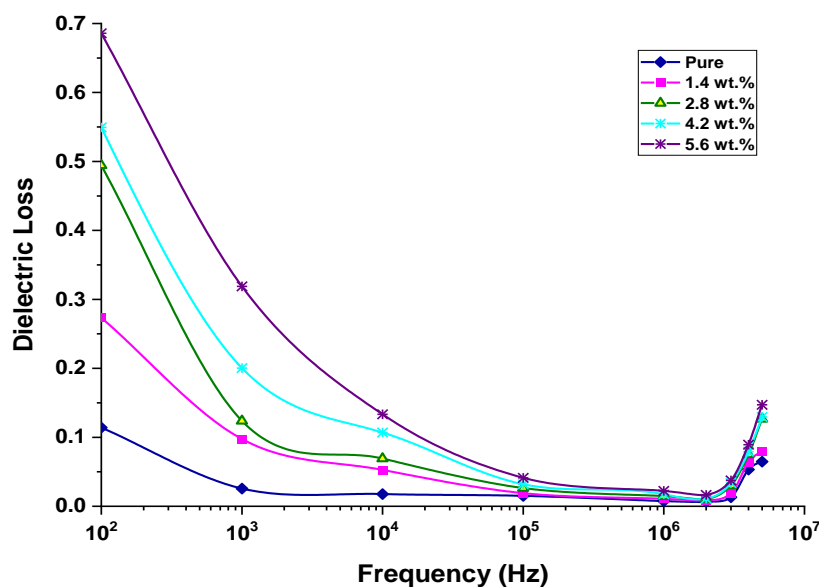


**Fig. 5.** Variation of dielectric loss for (PMMA -PC/Sb<sub>2</sub>O<sub>3</sub>-GO) Nanocomposites with frequency at room temperature.

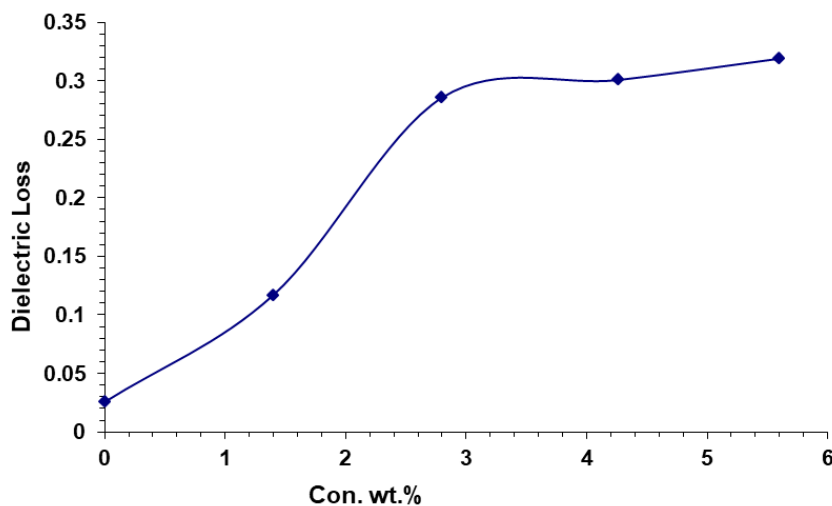


**Fig. 6.** Effect of(Sb<sub>2</sub>O<sub>3</sub> - GO) NPs content on dielectric loss for (PMMA- PC) blend at 100Hz.

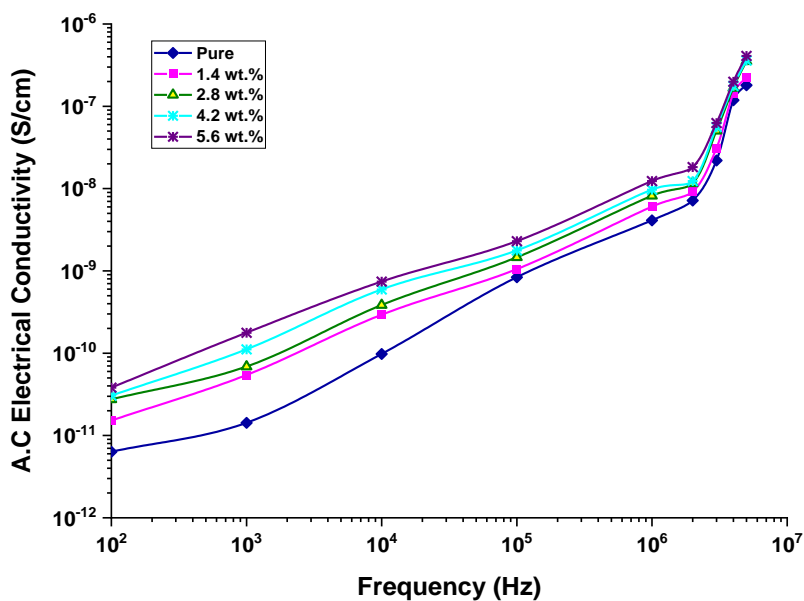


**Fig. 7.** Variation of A.C electrical conductivity for (PMMA -PC/Sb<sub>2</sub>O<sub>3</sub>-GO) nanocomposites with frequency at room temperature.

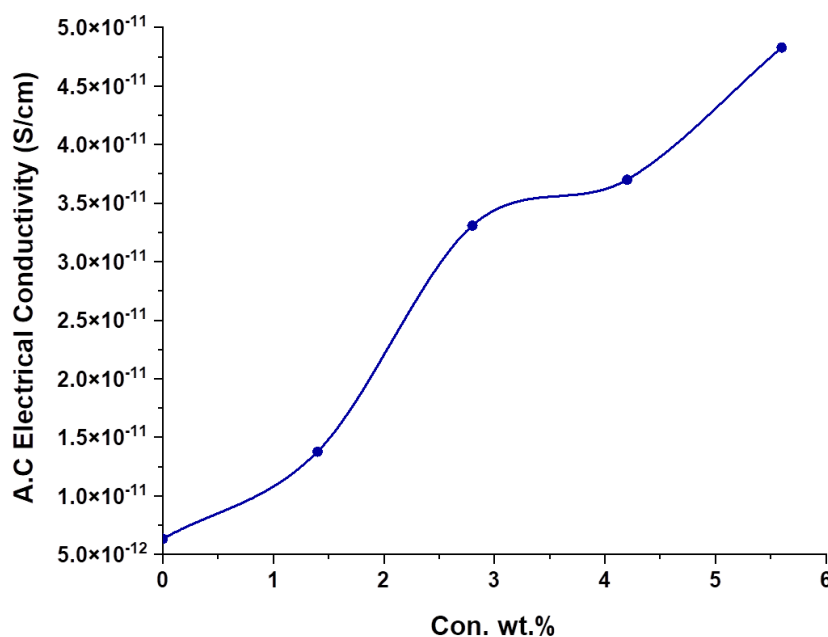


**Fig. 8.** Effect of ( $\text{Sb}_2\text{O}_3$ -GO) content on A.C electrical conductivity for (PMMA-PC) blend at 100Hz.

allowing for an increase in charge carriers [21-23]. As a result, the resistance of nanocomposite materials reduces, while A.C electrical conductivity rises. At high concentrations, the nanoparticles in the nanocomposites form a network, which is consistent with agree with [24,25].

## Conclusions

Flexible, lightweight and few cost films of (PMMA - PC/ $\text{Sb}_2\text{O}_3$ -GO) were prepared using the solution cast technique. The structure and dielectric properties of (PMMA -PC/ $\text{Sb}_2\text{O}_3$ -GO) films were studied to use in different electrical applications. SEM micrographs confirm the miscibility of polymers (PMMA -PC/ $\text{Sb}_2\text{O}_3$ -GO) in the blend. The growth of ( $\text{Sb}_2\text{O}_3$ -GO) in (PMMA -PC) blend was confirmed by the presence of irregular-

shaped granular microstructures. The FTIR spectra show the (PMMA-PC) blends did not indicate the existence of any chemical interaction the adding of ( $\text{Sb}_2\text{O}_3$  and GO) nanoparticles to the polymer blend results in two noteworthy alterations: modest changes in absorption band intensities and vibrational band intensities in peak at  $995.79 \text{ cm}^{-1}$  and  $749 \text{ cm}^{-1}$ . The dielectric constant, dielectric loss and A.C electrical conductivity rise as the content of ( $\text{Sb}_2\text{O}_3$ -GO) increases. The dielectric constant and dielectric loss reduce as frequency rises, although the A.C electrical conductivity increases. The results show that the nanocomposites (PMMA-PC/ $\text{Sb}_2\text{O}_3$ -GO) might be employed in a range of electronic applications.

**Sabur Dhay Ali** – PhD student;  
**Habeeb Majeed Ali** – PhD, Prof.;  
**Hashim Ahmed** – PhD, Prof.

- [1] A. Hashim, M. A. Habeeb, & A. Hadi, *Synthesis of novel polyvinyl alcohol–starch-copper oxide nanocomposites for humidity sensors applications with different temperatures*, Sensor Letters, 15(9), 758 (2017); <https://doi.org/10.1166/sl.2017.3876>.
- [2] A. Hazim, H.M. Abduljalil, & A. Hashim, *Analysis of Structural and Electronic Properties of Novel (PMMA/ $\text{Al}_2\text{O}_3$ , PMMA/ $\text{Al}_2\text{O}_3$ -Ag, PMMA/ $\text{ZrO}_2$ , PMMA/ $\text{ZrO}_2$ -Ag, PMMA-Ag) Nanocomposites for Low Cost Electronics and Optics Applications*, Trans. Electr. Electron. Mater. 21, 48 (2020); <https://doi.org/10.1007/s42341-019-00148-0>.
- [3] Kaoutar Benthami, Mai ME. Barakat and Samir A. Nouh, *Modification of optical properties of PC-PBT/ $\text{Cr}_2\text{O}_3$  and PC-PBT/ $\text{CdS}$  nanocomposites by gamma irradiation*, Eur. Phys. J. Appl. Phys., 92 (2), 20402 (2020); <https://doi.org/10.1051/epjap/2020200201>.
- [4] G.G. Politano, C. Versace, *Electrical and Optical Characterization of Graphene Oxide and Reduced Graphene Oxide Thin Films*, Crystals, 12, 1312 (2022); <https://doi.org/10.3390/cryst12091312>.
- [5] A. K. Jha, K. Prasad, and K. Prasad, *A green low-cost biosynthesis of  $\text{Sb}_2\text{O}_3$  nanoparticles*, Biochem. Eng. J., 43(3), 303 (2009); <https://doi.org/10.1016/j.bej.2008.10.016>.
- [6] T.A. Abdel-Baset, A. Hassen, *Dielectric relaxation analysis and Ac conductivity of polyvinyl alcohol/polyacrylonitrile film*, Physica B, 499, 24 (2016); <http://dx.doi.org/10.1016/j.physb.2016.07.002>.
- [7] P. Beena and H. S. Jayanna, *Dielectric studies and AC conductivity of piezoelectric barium titanate ceramic polymer composites*, Polymers and Polymer Composites, 27(9) 619 (2019); <https://doi.org/10.1177/0967391119856140>.

- [8] A. Qureshi<sup>1</sup>, A. Mergen<sup>1</sup> and B. Aktas, *Dielectric and magnetic properties of YIG/PMMA nanocomposites*, Journal of Physics: Conference Series, 153, 1 (2009); <https://doi.org/10.1088/1742-6596/153/1/012061>.
- [9] N.K. Abbas, M.A. Habeeb, and A.J.K. Algidsawi, *Preparation of chloro penta amine cobalt (III) chloride and study of its influence on the structural and some optical properties of polyvinyl acetate*, International Journal of polymer Science, 2015, 926789 (2015); <https://doi.org/10.1155/2015/926789>.
- [10] D.Vaishnav<sup>1</sup> and R. K. Goyal, *Thermal and Dielectric Properties of High-Performance Polymer/ZnO Nanocomposites*, IOP Conf. Series: Journal of Materials Science and Engineering, 64, 1 (2014); <https://doi.org/10.1088/1757-899X/64/1/012016>.
- [11] A. Srivastava, K. Kumar Jana, P. Maiti, D. Kumar, and O. Parkash, *Investigations on Structural, Mechanical, and Dielectric Properties of PVDF/Ceramic Composites*, Journal of Engineering, 2015, Article ID 205490, 9 (2015); <https://doi.org/10.1155/2015/205490>.
- [12] E .Abdelrazek, Elashmawi I, Hezma A, Rajeh A, Kamal M, *Effect of an encapsulate carbon nanotubes (CNTs) on structural and electrical properties of PU/PVC nanocomposites*, Phys B Condens Matter., 502, 48 (2016), <https://doi.org/10.1016/j.physb.2016.08.040>.
- [13] A .Rajeh, HM Ragab, MM Abutalib. *Co doped ZnO reinforced PEMA/PMMA composite: structural, thermal, dielectric and electrical properties for electrochemical applications*, J Mol Struct., 1217, 128447 (2020); <https://doi.org/10.1016/j.molstruc.2020.128447>.
- [14] S. Ju<sup>1</sup>, M. Chen<sup>1</sup>, H. Zhang and Z. Zhang, *Dielectric properties of nano silica/low-density polyethylene composites: The surface chemistry of nanoparticles and deep traps induced by nanoparticles*, Journal of express Polymer Letters, 8(9), 682 (2014), <https://doi.org/10.3144/expresspolymlett.2014.71>.
- [15] .Chakraborty, K. Gupta, D. Rana and A. Kumar Meikap, *Dielectric relaxation in polyvinyl alcohol–polypyrrole–multiwall carbon nanotube composites below room temperature*, Advances in Natural Sciences, 4, 1 (2014); <http://dx.doi.org/10.1088/2043-6262/4/2/025005>.
- [16] P. Vasudevan, S. Thomas, K. Arunkumar, S. Karthika and N. Unnikrishnan, *Synthesis and dielectric studies of poly (vinyl pyrrolidone) /titanium dioxide nanocomposites*, Journal of Materials, Science and Engineering, 73, 1, (2015); <https://doi.org/10.1088/1757-899X/73/1/012015>.
- [17] I. Tantis, G. Psarras and D. Tasis, *Functionalized graphene poly (vinyl alcohol) nanocomposites: Physical and dielectric properties*, Journal of express Polymer Letters, 6(4), 283 (2012); <https://doi.org/10.3144/expresspolymlett.2012.31>.
- [18] C. M. Mathew, K. Kesavan, and S. Rajendran, *Structural and Electrochemical Analysis of PMMA Based Gel Electrolyte Membranes*, International Journal of Electrochemistry, 2015, Article ID 494308, 7, (2015); <https://doi.org/10.1155/2015/494308>.
- [19] P. Pradeepa and M. Ramesh Prabhu, *Investigations on the Addition of Different Plasticizers in poly (ethylmethacrylate)/poly (vinylidene fluoride-co-hexa fluoro propylene) Based Polymer Blend Electrolyte System*, International Journal of Chemical Technology Research, 7(4), 2077 (2015);
- [20] M.A. Habeeb, A. Hashim, and A. Hadi, *Fabrication of New Nanocomposites: CMC-PAA-PbO<sub>2</sub> Nanoparticles for Piezoelectric Sensors and Gamma Radiation Shielding Applications*, Sensor Letters, 15(9), (2017); <https://doi.org/10.1166/sl.2017.3877>.
- [21] Hojjat and A. Mahmood and Borhani, *Effect of EVA Content upon the Dielectric Properties in LDPE-EVA Films*, International Journal of Engineering Research, 4 (2), 69 (2015); <https://doi.org/10.17950/ijer/v4s2/206>.
- [22] K. J. Kadhim, I. R. Agool, & A. Hashim, *Effect of zirconium oxide nanoparticles on dielectric properties of (PVA-PEG-PVP) blend for medical application*, Journal of Advanced Physics, 6(2), 187 (2017); <https://doi.org/10.1166/jap.2017.1313>.
- [23] O. Abdullah, G. M. Jamal, D. A. Tahir and S. R. Saeed, *Electrical Characterization of Polyester Reinforced by Carbon Black Particles*, International Journal of Applied Physics and Mathematics, 1 (2), 101 (2011); <https://doi.org/10.7763/IJAPM.2011.V1.20>.
- [24] N. Hayder, M.A. Habeeb, and A. Hashim, *Structural, optical and dielectric properties of (PS-In<sub>2</sub>O<sub>3</sub>/ZnCoFe<sub>2</sub>O<sub>4</sub>) nanocomposites*, Egyptian Journal of Chemistry, 63, 577 (2020), <https://doi.org/10.21608/EJCHEM.2019.14646.1887>.
- [25] Qayssar M. Jebur, Ahmed Hashim and Majeed A. Habeeb, *Fabrication, Structural and Optical Properties for (PolyvinylAlcohol–Polyethylene Oxide–Iron Oxide) Nanocomposites*, Egypt. J. Chem., 63(2), (2020); <https://doi.org/10.21608/ejchem.2019.10197.1669>.

Д.А. Сабур<sup>1</sup>, М.А. Хабіб<sup>2</sup>, А. Хашим<sup>2</sup>

## Виготовлення четвертинних наноструктур GO/Sb<sub>2</sub>O<sub>3</sub>/PMMA/PC та адаптація їх структурних і діелектричних характеристик для твердотільних електронних нанопристроїв

<sup>1</sup>Кафедра оптичної техніки, Університетський коледж Аль-Мустакбал, Вавилон, Ірак

<sup>2</sup>Вавилонський університет, Освітній коледж чистих наук, факультет фізики, Ірак, [ahmed\\_tay@yahoo.com](mailto:ahmed_tay@yahoo.com)

Плівки четвертинних наноструктур (PMMA-PC/Sb<sub>2</sub>O<sub>3</sub>-GO) отримано методом лиття з різними концентраціями НЧ Sb<sub>2</sub>O<sub>3</sub>/GO (0, 1,4 %, 2,8 %, 4,2 % та 5,6 %). Структурні та діелектричні характеристики системи наноструктур (PMMA-PC/Sb<sub>2</sub>O<sub>3</sub>-GO) досліджували для їх використання в різних нанопристроях твердотільної електроніки. Морфологію плівок наноструктур (PMMA-PC/Sb<sub>2</sub>O<sub>3</sub>-GO) досліджено за допомогою скануючої електронної мікроскопії (SEM). SEM-зображення вказують на велику кількість однорідних і когерентних агрегатів або шматків. Аналіз інфрачервоної спектроскопії з перетворенням Фур'є (FTIR) проводили, щоб показати взаємодію між Sb<sub>2</sub>O<sub>3</sub>/GO NP та сумішшю PMMA/PC. Досліджено діелектричні властивості плівок наноструктур в діапазоні частот (100Гц-5МГц). Показано, що діелектрична проникність, діелектричні втрати та електропровідність змінного струму зростають зі збільшенням концентрації НЧ (Sb<sub>2</sub>O<sub>3</sub>-GO). Діелектрична проникність і діелектричні втрати були зменшені, тоді як електрична провідність зростала з частотою. Результати показали, що наноструктури PMMA-PC/Sb<sub>2</sub>O<sub>3</sub>-GO можна розглядати як перспективні матеріали для твердотільних електронних нанопристроїв.

**Ключові слова:** нанокompозити, оксид графену, діелектричні властивості, суміш, нанопристрої.